

1 *Supporting Information*

2 **Variations of the density of ambient black carbon retrieved by a new**
3 **method: importance to CCN prediction**

4
5 **Jingye Ren^{1,2}, Fang Zhang^{2*}, Lu Chen¹ Jiexiao Liu¹**

6
7 *¹College of Global Change and Earth System Science, Beijing Normal University,*
8 *Beijing 100875, China*

9 *²School of Civil and Environmental Engineering, Harbin Institute of Technology*
10 *(Shenzhen), 518055 Shenzhen, China*

11
12 **Correspondence to: Fang Zhang (zhangfang2021@hit.edu.cn)*

13
14 **Contents of this file**

15 **Methods and theory for CCN number concentration prediction**

16 **Figure S1, S2, S3, S4**

17

18

19

20

21

22

23 **Methods and theory for CCN number concentration prediction**

24 **Assumption 1: BC internally mixed**

25 BC particles are assumed to be internally mixed with bulk chemical composition,
26 when using a density of BC with the value of 2.1 g cm^{-3} in the sensitivity test. For this
27 scheme, six species are considered, ie., NH_4HSO_4 , $(\text{NH}_4)_2\text{SO}_4$, NH_4NO_3 , POA, SOA
28 and BC. By applying the hygroscopicity parameter κ_{chem} into κ -Köhler relationship
29 (Petters & Kreidenweis, 2007), the critical diameter or activation diameter (D_{cut}) can be
30 obtained at a given supersaturation (S). Thus, the CCN concentration can be predicted
31 by using the critical diameter and particle number size distribution.

32 The equations used in the estimating N_{CCN} are as follows,

$$33 \quad \text{CCN}_{pre} = \int_{D_{cut}}^{D_{end}} n(\log D_p) d \log D_p \quad (1)$$

34 where D_{cut} is the critical diameter, D_{end} is the upper size limit of the particle number
35 size distribution (PNSD), $n(\log D_p)$ is the function of the aerosol number size
36 distribution.

$$37 \quad D_{cut} = \sqrt[3]{\frac{4A^3}{27\kappa \ln^2 S}}, \quad A = \frac{4\sigma_{s/a} M_w}{RT\rho_w} \quad (2)$$

38 Where κ is the hygroscopicity parameter, S is a given supersaturation, M_w is the
39 molecular weight of water, $\sigma_{s/a}$ is the surface tension of pure water, ρ_w is the density of
40 water, R is the gas constant, and T is the absolute temperature.

41 **Assumption 2: BC externally mixed**

42 When using a density of 0.14 g cm^{-3} in the sensitivity test, BC particles are
43 assumed to be externally mixed but other five species are treated as internally mixed,

44 ie., NH_4HSO_4 , $(\text{NH}_4)_2\text{SO}_4$, NH_4NO_3 , POA and SOA. The CCN number concentration
45 of the internal mixture is denoted as $N_{\text{CCN_In}}$. The way to retrieve the critical diameter
46 (D_{cut}) is same as the assumption 1. The difference is that the $N_{\text{CCN_In}}$ should be
47 multiplied by the volume fraction of the internal mixed particles to get the finally N_{CCN}
48 (Ren et al., 2018). The CCN concentration can be calculated as follows:

$$49 \quad CCN_{pre_IN} = \left(\int_{D_{cut}}^{D_{end}} n(\log D_p) d \log D_p \right) \cdot VF \quad (3)$$

50 Where VF is the volume fraction of the internally mixed components. The other
51 parameters are same as those presented in Eqs. 1-2.

52 **Assumption 3: aged BC internally mixed but fresh BC externally mixed**

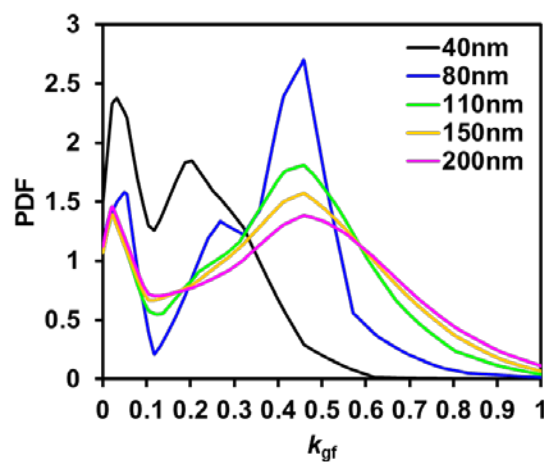
53 In this assumption, the fresh BC and POA are externally mixed but sulfate, nitrate
54 and SOA with the aged BC particles are internally mixed. The mass fraction of
55 internal/aged BC and external/fresh BC are retrieved from 2.2. Similar to the
56 assumption 2, the CCN concentration is calculated by using the critical diameter and
57 the PNSD. And the CCN number concentration also should be multiplied by the volume
58 fraction of five internal species. The equation is the same as Eqs. 3. The other
59 parameters are same as those presented in Eqs. 1-3. By varying the densities of internal
60 and external BC particles, a CCN closure test has been done based on this assumption.
61 Then the optimal density of internal and external BC is obtained when the best estimates
62 of N_{CCN} are achieved.

63 **References**

64 Petters, M. D., & Kreidenweis, S. M.: A single parameter representation of hygroscopic
65 growth and cloud condensation nucleus activity, *Atmospheric Chemistry and Physics*,
66 7(8), 1961-1971, <https://doi.org/10.5194/acp-7-1961-2007>, 2007.

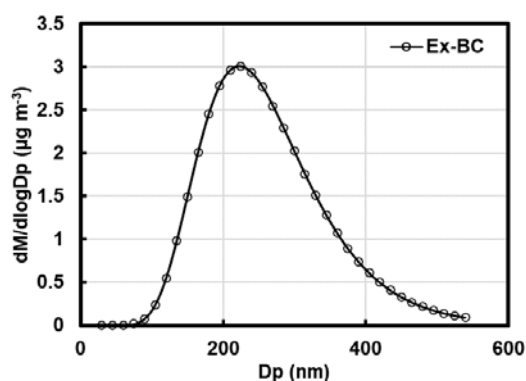
67 Ren, J., Zhang, F., Wang, Y., Collins, D., Fan, X., Jin, X., et al.: Using different
68 assumptions of aerosol mixing state and chemical composition to predict CCN
69 concentrations based on field measurements in urban Beijing, Atmospheric
70 Chemistry and Physics, 18, 6907–6921, <https://doi.org/10.5194/acp-18-6907-2018>,
71 2018.
72 Xie, Y.Y., Ye, X.N., Ma, Z., Tao, Y., Wang, R.Y., Zhang, C., et al.: Insight into winter
73 haze formation mechanisms based on aerosol hygroscopicity and effective density
74 measurements, Atmospheric Chemistry and Physics, 17(11), 7277-7290,
75 <https://doi.org/10.5194/acp-17-7277-2017>, 2017.

76 **Figures**



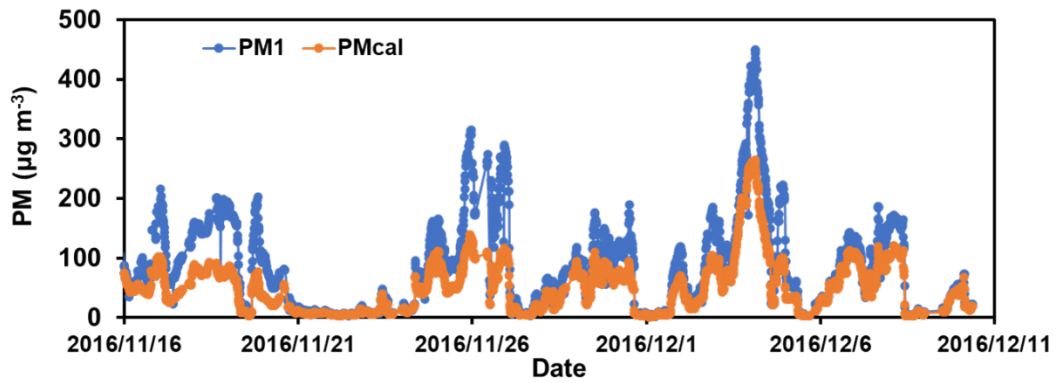
77

78 **Figure S1.** Average κ -PDF patterns of particles in different sizes.



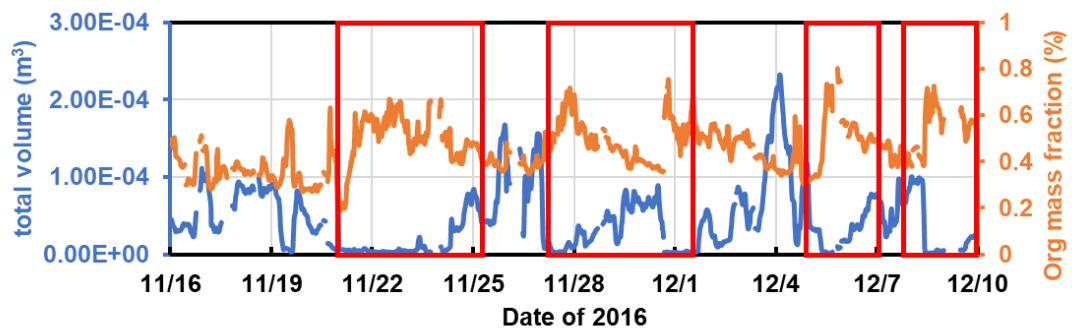
79

80 **Figure S2.** Average mass size distribution of Ex-BC by modeling as a single log-normal
81 distribution.



82

83 **Figure S3.** Temporal evolutions of PM_1 concentration (measured with an Aerosol
 84 Chemical Speciation Monitor, ACSM and calculated PM_{cal} (measured with a scanning
 85 mobility particle sizer, SMPS). The effective density of PM_1 was assumed to be 1.5 g
 86 cm^{-3} in the range of 10–550 nm measured (Xie et al., 2017).



87

88 **Figure S4.** Time series of the calculated total volume of PM_1 and mass fraction of
 89 organics.